Development and Evaluation of Gamut Extension Algorithms

Justin Laird,[1]* Remco Muijs,[2] Jiangtao Kuang[3]

[1] The Gunlocke Co., Wayland, NY 14572

[2] Video Processing Systems Group, Philips Research Europe, Eindhoven, The Netherlands

[3] Omnivision, Sunnyvale, CA 94089

Received 30 April 2007; revised 3 July 2008; accepted 30 July 2008

Abstract: In recent years, new display technologies have emerged that are capable of producing colors that exceed the color gamut of broadcast standards. On the other hand, most video content currently remains compliant with the EBU standard and as such, there is a need for color mapping algorithms that make optimal use of the wider gamut of these new displays. To identify appropriate color mapping strategies, we have developed, implemented, and evaluated several approaches to gamut extension. The color rendering performance and robustness to different image content of these algorithms were evaluated against a reference (true-color) mapping. To this end, two psychophysical experiments were conducted using a simulated and actual wide-gamut display. Results show that the preferred algorithm had a dependency on image content, especially for images with skin tones. In both experiments, however, there was preference shown for the algorithm that balances chroma and lightness modulations as a function of the input lightness. The newly designed extension algorithms consistently outperformed true-color mapping, thus confirming the benefit of appropriate mapping on wide-gamut displays. © 2009 Wiley Periodicals, Inc. Col Res Appl, 34, 443–451, 2009; Published online in Wiley InterScience (www.interscience.wiley.com). DOI 10.1002/col.20537

Key words: LC TV; wide gamut; color processing; psychophysical experiment

INTRODUCTION

The imaging world is inundated with numerous types of displays, recorders, and printing devices, all of which rely heavily on color. In order for these devices to be successful they must handle colors properly, which includes the ability to transfer colors from one device to another. A classic example is the transfer of colors shown on a desktop monitor to a printer such that the colors in the final print and those on the monitor match. This example of color management has been extensively researched[1,2] and implemented successfully in industry, as illustrated by the proliferation of the desktop publishing market.

The range of colors produced for a given device is defined by the chromaticity and maximum luminance of the primaries, where a display typically has three colors [red, green, and blue (RGB)] and a printer typically has four colors (cyan, magenta, yellow, and black). This range of colors produced by a device is known as the "device color gamut", and the method of transferring colors between devices is referred to as gamut mapping.[1,2] We follow the convention for distinguishing two types of gamut mapping: compression and extension. Gamut compression refers to mapping colors from a source that has a larger gamut to a destination that has a smaller gamut, as would happen when mapping from a monitor to a printer. Conversely, gamut extension refers to mapping colors from a smaller source gamut to a larger destination gamut.

In the television industry, the signal that reaches the display has been encoded using primaries specified by the European Broadcasting Union (EBU) standard (also referred to as Rec. 709).[3] Previously, most display gamuts fit within or were approximately the same size as the EBU gamut. However, because of technological advances in the display industry, displays that can produce colors outside the source EBU standard are on the market. An

*Correspondence to: Justin Laird (e-mail: lairdj@gunlocke.com).

example of gamut extension is then mapping from EBU encoded video to a wide-gamut (WG) display. A display is referred to as "WG" if it is capable of producing colors outside the EBU gamut. These WG displays have been realized by using more than three primaries,[4–6] also referred to as multiprimary displays. Another method for achieving a wide-color gamut is to use more saturated light sources, such as the narrow spectral radiance of light-emitting diodes (LEDs).[7,8] In spite of the recent advances in transmission standards, such as the recently proposed xvYCC standard,[9] video signals with colors outside the EBU gamut have yet to become widespread. As a result, gamut mapping is needed between the EBU source material and the WG display. In other words, the current topic of consideration is how to best use the additional space of the larger device gamut. As gamut extension is primarily aimed at enhancing the appearance of an image, its performance should be evaluated in terms of observer preference rather than color reproduction accuracy.

A number of extension methods have been developed in the past and utilized in various applications. This article focuses on a few that were most pertinent in this research. Kang *et al.*[10] analyzed preferred gamut compression and extension methods by using an observer-central experimental tool. In a series of subjective experiments, participants were asked to modify the colors of an image to arrive at an image of their preference. A final extension algorithm was developed by fitting a numerical model to the experimental data and consisted of a linear lightness and chroma mapping. This research showed that mapping colors along a lightness and chroma direction could be beneficial for extension algorithms.

Kotera *et al.*[11] proposed a method to recover either degraded colors taken under insufficient illumination or faded colors after long preservation in prints. In addition to color recovery, gamut extension can be employed to make the image more vivid. The latter is achieved using histogram specification, which extends separately the histograms of luminance and chrominance in the YCC color space. The histogram of the original luminance, Y, is normalized and redistributed to form a Gaussian distribution covering a wider luminance range than the input. The image colors are binned in luminance sectors and hue slices, and the same procedure is subsequently applied to the data in each individual bin.

Kim *et al.*[4] discussed three possible gamut extension directions in which to extend an EBU standard signal to a WG multiprimary display. Their method utilizes directional mapping in both lightness and chroma. The extension strategies and parameters have been designed specifically for mapping to one type of multiprimary display and may provide suboptimal results when applied to displays with different gamuts.

The aforementioned algorithms are novel and innovative approaches to gamut extension. However, in some cases, the research lacks only in the subjective quality evaluation of the algorithms and in others, it is relevant only for a specific WG display. In this context, a more generalized framework and evaluation for mapping colors to WG displays is desirable. In this article, several generic approaches to gamut extension will be outlined and their color rendering performance will be subjectively evaluated with respect to a colorimetric mapping in a series of psychophysical experiments.

EXPERIMENTAL: GAMUT EXTENSION ALGORITHMS

On the highest level, the aim of gamut mapping is to ensure a good correspondence of overall color appearance between the original and the reproduction by compensating for the mismatch in the size, shape, and location between the original and reproduction gamuts.[1] In general, the algorithms presented here can be applied in many situations. However, we used them to map colors from a smaller source gamut (the EBU standard[3]) to a larger destination gamut (a wide-color gamut, LED-backlit TV). The differences between the gamuts are visualized in Fig. 1, where the EBU standard and WG display are shown in color and wire-frame, respectively. The WG display has red and green primaries that are more saturated than EBU with the largest difference in the green primary. The blue primary of the display is quite similar to that of EBU.

Two of the gamut extension algorithms (GEAs) below are implemented in a perceptually uniform color space, because it is desirable to modify perceptual attributes such as lightness, chroma, and hue separately and independently. It is also considered necessary to know precisely which attributes of color are being changed and by how much. This is best accomplished through a more perceptually uniform color space such as CIELAB.[12]

As a first step to explore color mapping in terms of gamut extension, the following five extension algorithms, are explained in more detail: 1. True-color, 2. Same drive signal (SDS), 3. Hybrid color mapping (HCM), 4. Chroma, and 5. Lightness-chroma adaptive.

The true-color algorithm maintains the color information between the original and the reproduction media, that is, without any gamut extension. Hence, this algorithm serves as a reference solution for the other GEAs. Comparing the performance of the other GEAs against this reference solution provides insight in the benefit of the WG feature as well as the impact of the associated color mapping methods. The implementation corresponds to the International Color Consortium (ICC)[13] color management process, where the *RGB* values from the source space are converted to *RGB* values of the destination space through the colorimetric intent:

$$\begin{bmatrix} R \\ G \\ B \end{bmatrix}_{\text{Destination}} = A^{-1}_{\text{Destination}} A_{\text{source}} \begin{bmatrix} R \\ G \\ B \end{bmatrix}_{\text{source}}, \qquad (1)$$

where A_{Source} is a 3×3 matrix with each column corresponding to the *XYZ* value of the primaries for the source,

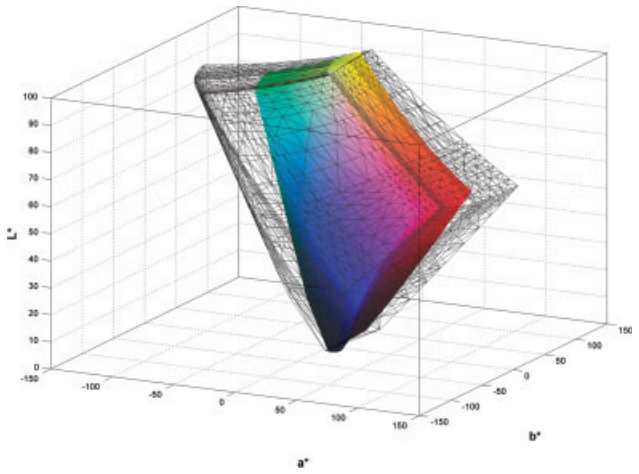

FIG. 1. EBU (color) and wide-gamut LC-TV (wire-frame) in CIELAB color space.

and $A^{-1}_{\text{Destination}}$ is the inverse of the 3×3 *XYZ* matrix of the destination primaries. The source *RGB* drive values are linearized using appropriate gamma functions and converted to *XYZ* using A_{Source}. The *XYZ* values are converted back to linear *RGB* using $A^{-1}_{\text{Destination}}$, and finally appropriate gamma functions are applied to transform the linear *RGB*s to corresponding destination-*RGB* values. Figure 2 shows a flowchart of the true-color mapping procedure.

The SDS algorithm is the simplest GEA used to extend content from a small color gamut (SG) to a wide-color gamut display. In this case, the original driving signal is directly applied to the display without any additional color processing. Consequently, the *RGB* primaries of the original gamut are mapped to the *RGB* primaries of the display, making full use of the wide-color gamut of the display (implicitly involving linear extension of the colors). It should be noted, however, that in the presence of hue differences between the input and reproduction primaries, this approach would inherently introduce hue shifts in the rendered images.

The HCM algorithm is based on concepts that were originally conceived for gamut compression. It involves a saturation-dependent linear combination of the true-color and SDS algorithms:

$$\begin{bmatrix} R \\ G \\ B \end{bmatrix}_{\text{HCM}} = (1-\alpha)\begin{bmatrix} R \\ G \\ B \end{bmatrix}_{\text{C}} + \alpha \begin{bmatrix} R \\ G \\ B \end{bmatrix}_{\text{SDS}}, \qquad (2)$$

where $[RGB]_{\text{HCM}}$ represents the *RGB* drive values after mapping; α is a piece-wise linear function that increases with saturation [as shown in Fig. 3(a)] and acts as a simple mixing function between true-color and SDS. $[RGB]_{\text{C}}$ and $[RGB]_{\text{SDS}}$ correspond to the colorimetric (or true-color) and SDS output signals, respectively. Consequently, HCM reverts to true-color mapping for low-saturated colors, whereas colors with higher saturation are increasingly mapped using the SDS-type extension. This is shown in Fig. 3(b) by the dotted curved line. This implies that the hue of highly saturated colors is transformed toward the *RGB*-primaries of the reproduction gamut, whereas for unsaturated, natural colors the hue is preserved. As such, this approach also enables the full range of the wide reproduction gamut to be exploited. It should be noted that this method partly operates in a device-dependent color space, and hence its performance depends on the relative shapes of the source and reproduction gamuts.

The last two algorithms require knowledge of the input and output gamut boundaries[14] and are implemented in the CIELAB color space. These GEAs are designed to make full use of the reproduction gamut, such that colors on the original gamut boundaries are always mapped to the reproduction gamut boundaries, and the colors inside the gamut are mapped correspondingly in a particular manner. It is important to note that the gamut be represented in a 3D color space, such as CIELAB, seen in Fig. 1, and not simply a 2D projection, as in a chromaticity diagram.[2] Once input and output gamut boundaries have been determined, a GEA can be implemented through modifications of color attributes, such as hue, chroma, lightness, and saturation. In CIELAB hue, chroma, and lightness are denoted by h, C^*, and L^* respectively.

The implementation of the last two algorithms is defined in terms of an extension direction and an extension type. The extension direction defines the ratio between the color attribute changes while mapping to a

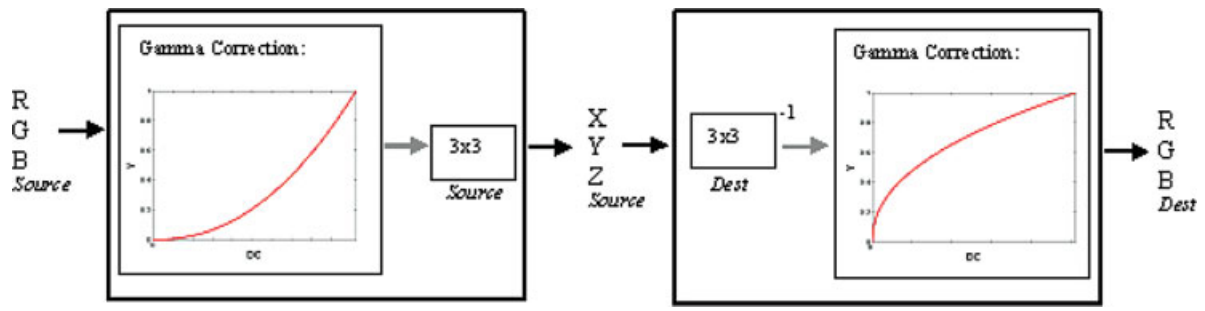

FIG. 2. Flowchart of true-color mapping where the input *RGB* drive values are first converted to linear *RGB* using an appropriate gamma function and then converted to *XYZ* using the 3×3 matrix of the source space. These *XYZ* values are converted back to linear *RGB* using the inverse 3×3 matrix of the output color space and an appropriate gamma function is applied to get final *RGB* values of the output space.

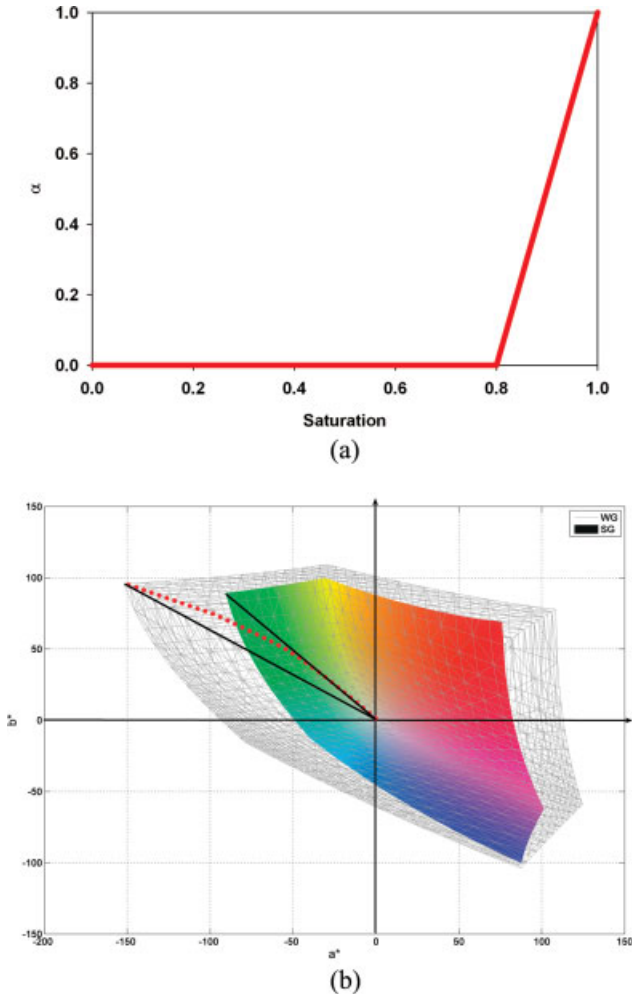

FIG. 3. (a) The mixing factor α [Eq. (2)] as a function of saturation; (b) Projection on the a^*b^* plane of HCM. Shown are the input and reproduction gamuts where the red dotted line illustrates how it increasingly maps toward a primary.

wider gamut. For each input color, it therefore defines the trajectory within a particular 3D color space along which the input colors are mapped. The chroma and lightness-chroma adaptive GEAs both maintain hue and modify exclusively the lightness and/or chroma components of color. The extension directions employed by the chroma and lightness-chroma adaptive mappings are illustrated using arbitrary gamuts in Figs. 4 and 5, respectively.

The chroma GEA maps colors along a direction of constant lightness and hue, only extending along the chroma axis, as illustrated in Fig. 4. The direction of the lightness-chroma adaptive extension, in Fig. 5, varies with the lightness of the original color, keeping the hue constant and altering both lightness and chroma. This method was inspired by the work of Kim *et al.*,[4] who proposed a functional behavior for the extension angle in the lightness-chroma plane, with low angles for low-lightness values and high angles for high-lightness values. However, for the lightness-chroma adaptive GEA used in this research the mapping-angle function is altered to incorporate both negative and positive angles with the turning point around $L^* = 50$, as seen in Fig. 6. Since the lightness values can be mapped downward, the lightness-chroma adaptive GEA includes contrast enhancement along with chroma boost. For midtone colors, the algorithm predominantly increases the chroma, thus making optimal use of the width of the reproduction gamut. For bright and dark (unsaturated) colors, this method mainly changes lightness, thus enhancing contrast. To avoid a lightness discontinuity around the middle lightness-values of the image, which are easily perceived by human viewers, the extension angle is set to zero (for a range of L^* around 50), as seen in Fig. 6.

In addition to an appropriate extension direction, the optimal extension type needs to be defined. The type of extension determines the mapping of the colors along a given trajectory (direction) in either a linear or a nonlinear manner. The extension type is expressed by a gain curve, which plots normalized distances of the input and output gamuts such that 1 refers to the gamut boundary and 0 refers to the achromatic (lightness) axis. Using this gain curve, the normalized distance of the input pixel to the input gamut boundary is transformed into a normalized distance to the output gamut boundary for the mapped pixel. Several transfer curves were tested in a pilot experiment and Fig. 7 shows the final transfer curve utilized for both the chroma and lightness-chroma adaptive extension directions and is referred to as a "high chroma boost" (HCB) design. In this figure, $C^*_{i(Max)}$ and $C^*_{r(Max)}$ represent the normalized maximum chroma of the input and the reproduction gamut, respectively. The lower solid line merely serves as a reference; it signifies a one-to-one mapping to the same chroma value, which corresponds to a true-color mapping and does not apply any gamut extension. The upper dotted line corresponds to a simple linear mapping (such as SDS). To avoid desaturation of the colors, the HCB extension type consistently maps colors at or above the true-color (bottom) curve.

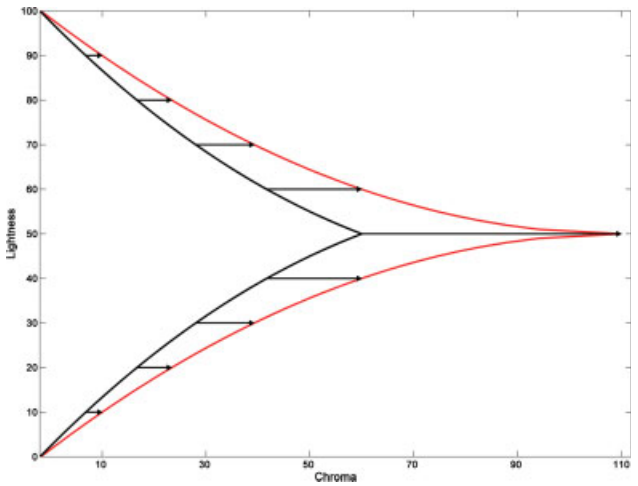

FIG. 4. Extension in the chroma direction for a given gamut. Note: The chroma values are shown only as an example.

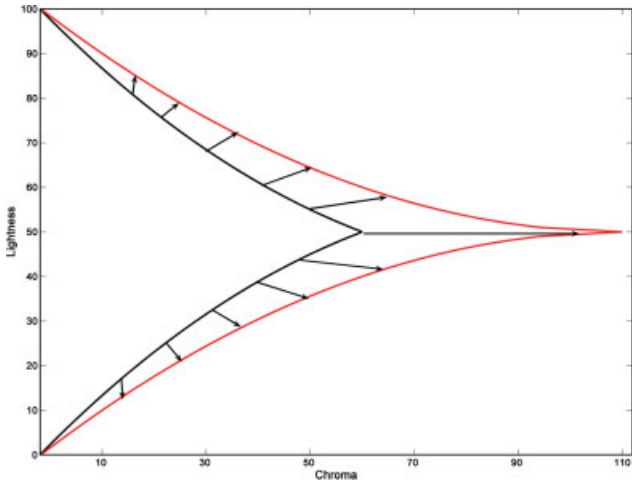

FIG. 5. Adaptive extension in both the lightness and chroma direction. Note: The chroma values are shown only as an example. [Color figure can be viewed in the online issue, which is available at www.interscience.wiley.com.]

The HCB method boosts high chroma colors more than low chroma colors to preserve the colors of natural objects and prevent coloring of achromatic content. The rationale behind this approach is that natural-object colors commonly have low to moderate chroma values, whereas the highest chroma values are often associated with unnatural objects, such as plastics, animations, etc. The idea for this approach was to preserve natural (memory) colors and extend more saturated, unnatural colors into the additional volume of the reproduction gamut.

Because the human visual system is very sensitive to hue changes, gamut mapping algorithms are often designed to be hue preserving. Out of the algorithms considered in this work, the true-color, chroma and adaptive GEAs preserve hue (thus eliminating one of the three dimensions of color and reducing a 3D mapping to a 2D mapping), while SDS and HCM may introduce hue shifts. The chroma and lightness-chroma adaptive GEAs operate exclusively on the input lightness and chroma coordinates while explicitly preserving hue.

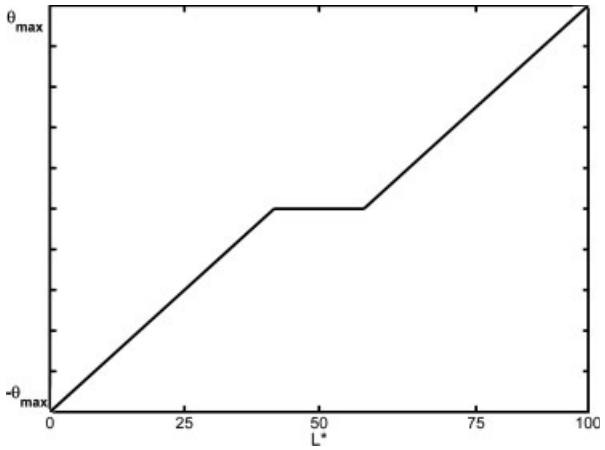

FIG. 6. The extension angle θ in the lightness-chroma plane, as a function of L^*.

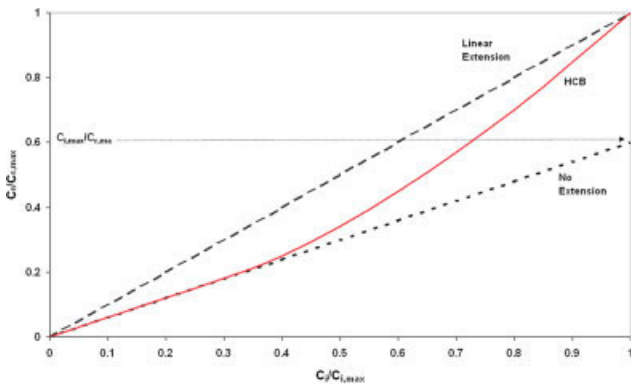

FIG. 7. HCB extension type, which effectively boosts colors having high-chroma values more than those with low-chroma values. $C_{i(max)}$ and $C_{r(max)}$ represent the chroma coordinates of the intersection points along the selected trajectory of the original and reproduction gamuts, respectively. [Color figure can be viewed in the online issue, which is available at www.interscience.wiley.com.]

EXPERIMENTAL: DESIGN

The performances of the five GEAs described in the previous section were evaluated in two psychophysical experiments, referred to as experiments A and B. Because actual WG displays were initially unavailable, experiment A utilized a simulated wide-color gamut display. Experiment B made use of an actual wide-color gamut display to determine if observers would fully appreciate the difference in image quality from different mappings on a wide-color gamut display over a standard EBU display. The robustness to image content of the same five algorithms on an actual WG display was also analyzed. Before each experiment, a pilot study was carried out by a tuning experiment using a small set of scenes, where each scene had multiple versions generated from different parameter values of the chroma and lightness-chroma adaptive algorithms. Observers selected the scene-version they preferred most and the corresponding parameter value was recorded. The parameter value that resulted in the most selected image was used in the algorithms.

Experiment A

The color gamut of a 40″ WG LC-TV incorporating a LED backlight was used as the desired output gamut for both experiments. In experiment A, this gamut was modeled through simulation. The color-mapping workflow started from a SG within EBU and was extended to the full EBU gamut. The relative gamut shape and volume ratio between the small gamut and the EBU gamut was identical to that of EBU and WG LC-TV gamuts, as illustrated in Fig. 8 on a chromaticity diagram. To obtain the positions of the SG primaries, the EBU primaries were scaled inward by the same ratio that the EBU primaries differ from the WG LC-TV. To prevent any difference in appearance resulting from differences in the white point

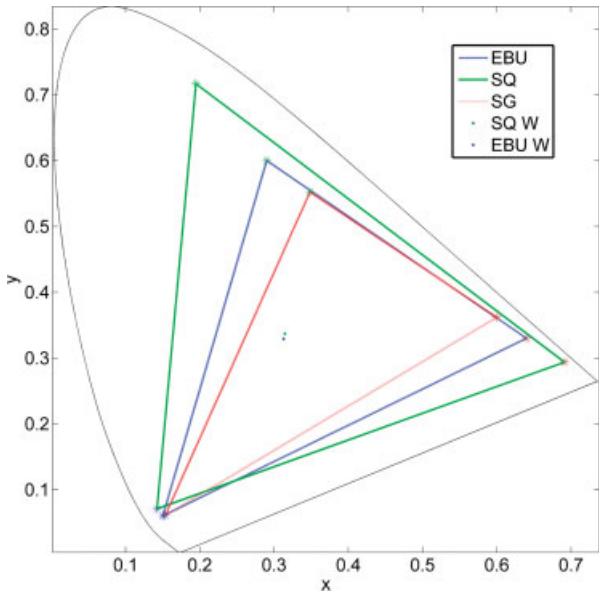

FIG. 8. Simulation of wide-color gamut display. The solid green line represents the wide-gamut display; the outer dotted line represents the EBU standard and the inner dotted line represents the small-gamut display used in experiment A. The white points were approximately the same (within 1 JND).

or the surround, the white point of both the original signal and the reproduction display were set to D65 under the same viewing conditions and with both displays having the same luminance values. Figure 8 shows the color gamuts of the simulated SG, a typical EBU-compliant display and the WG LC-TV projected onto the 2D CIExy chromaticity diagram.

The experiment was carried out on a characterized 20″ Philips EBU standard CRT display. The maximum luminance of the display was set to 117 cd/m^2, and a white point of 6500 K was selected. Observers viewed images at a distance of ~60 cm (24″) from a display with a dim surround and a 20% gray background. The 10 test images for experiment A, shown in the first two rows of Fig. 9, included: outdoor scenes containing the majority of hues and including memory colors, such as sky, trees, earth, etc; two facial portraits to evaluate skin tone reproduction; one image served to test the color reproduction of fruit; images that contained unnatural colors, such as plastic materials; and a computer generated scene that contained both memory and nonmemory colors. The images used in experiment A were chosen such that 99.9% of the colors fell within the SG gamut so that minimal clipping was required before extension. There were 25 color normal observers for this experiment. The GEAs' performance was evaluated using a paired-comparison psychophysical experiment. Subjects selected the image they preferred out of a pair of simultaneously displayed images. For each image, observers were shown all possible combinations of the five GEAs. Since there were 5 algorithms and 10 scenes, each observer had 100 total comparisons to judge. Before the experiment, each observer viewed a set of training images to familiarize them with the type and level of variations in the stimuli. To factor out any bias, the order of images shown and the location (left or right) of the images were randomized per observer.

Experiment B

Experiment B was conducted on a characterized 40″ LC TV with a 6500 K white point and a maximum luminance of 310 cd/m^2. This display was previously characterized using known techniques to build a characterization model[11,15] with the results shown in Table I.

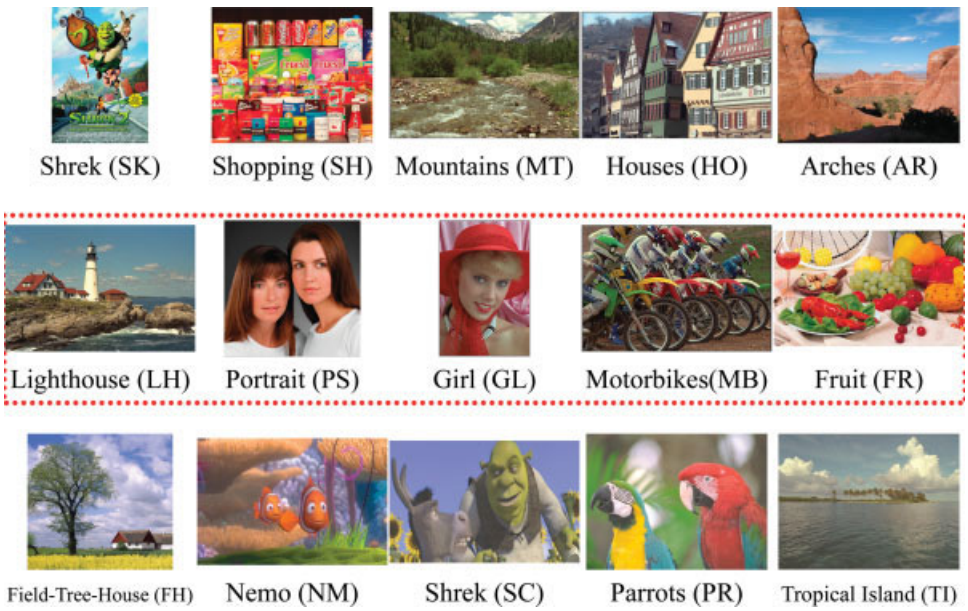

FIG. 9. Image content used in the psychophysical experiments. The images in rows 1 and 2 were used in experiment A, whereas the images in rows 2 and 3 were used in experiment B. Note that images in row 2, highlighted by the red dotted line were used in both experiments.

TABLE I. Results of characterization model for the LC-TV using 2060 random RGB colors.

	Average	Maximum	Minimum	Standard deviation
ΔE_{00}	0.88	2.77	0.01	0.00

All observers sat 3 m (118″) from the center of the TV with a uniformly lit, dim surround in an otherwise darkened room. The set of images for experiment B used five from A and five other images seen in rows 2 and 3 in Fig. 9. Since this experiment used a different display than previous, images with more saturated content were used in addition to images that were well within the EBU gamut. As in experiment A, images were shown on the display having a 20% gray background in a dim surround. There were also 25 color normal observers in this experiment, and all other experimental procedures were the same as in experiment A. Figure 10 shows the setup of experiment B from the viewpoint of the observer.

RESULTS

The data in both the experiments was analyzed using Thurstone's Law of Comparative Judgment, Case V[15] together with the procedure described by Rajae-Joordens and Engel.[16] The data from the paired-comparison experiments yield preference percentages, which can be transformed to interval scales using Thurstone's method. The Joordens-Engel method utilizes a Generalized Linear

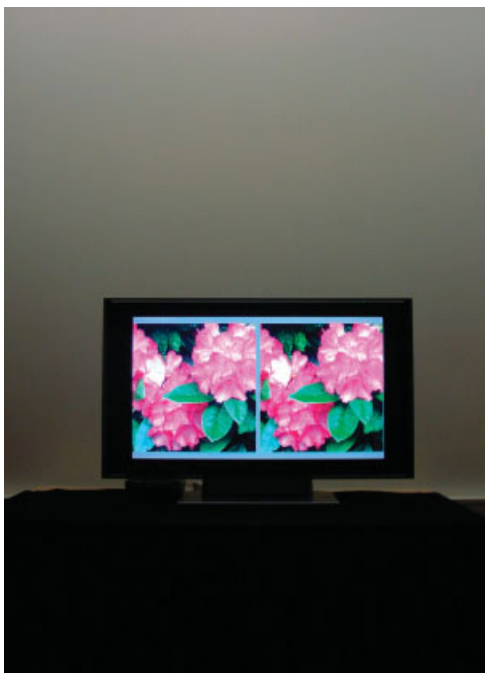

FIG. 10. Setup of subjective experiment. There is a uniform, neutral light shining on the wall from the ceiling so that the brightness of the surround decreases approaching the floor. There are two images on the screen with a background of medium gray. A gray bar that is the same color as the background separates the images.

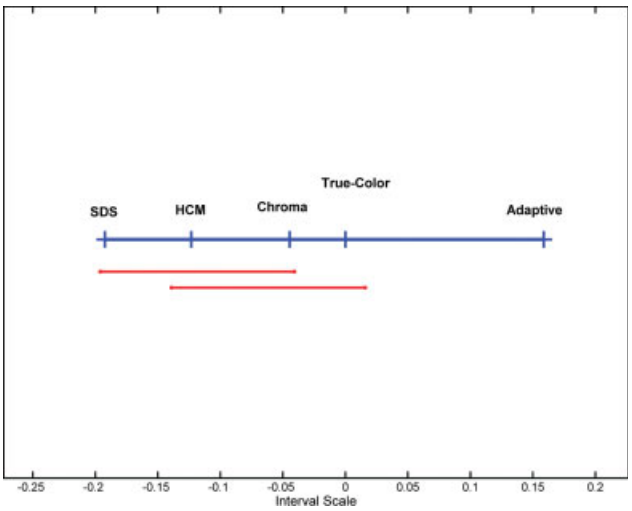

FIG. 11. Results for all images and observers in experiment A. The underlined portion represents algorithms that are not statistically different from each other. In this figure, the lightness-chroma adaptive algorithm is statistically different (and preferred all others). However, the differences amongst the algorithms are relatively small (the maximum interval scale value is about 0.15).

Model (GLM) regression model analysis[16] on the data to test for significant effects. To test whether the Thurstone Case V model fits the data sufficiently well, the average absolute deviation (AAD) was computed between the predicted and observed preference proportions. For the data shown in Fig. 11, the AAD of the proportions results in an error of 0.037, indicating that the Case V model is applicable for this experiment. Figure 11 shows algorithm preference (labeled interval scale) averaged over all participants and image content for experiment A. The interval scale values are shifted in such a manner that the value of the true-color algorithm, which represents a reference solution, is equal to zero. In Fig. 11 (as well as Fig. 13), the underlined portion of the scale represents differences that were tested using the GLM analysis and found not to be statistically significant. Figure 11 shows that the lightness-chroma adaptive algorithm is statistically different from true-color and preferred over the other algorithms. This figure also indicates that SDS was statistically different and not preferred to true-color and was the least preferred algorithm overall. Using the cumulative normal distribution with a mean of 0 and a standard deviation of 1, percentages can be calculated from the interval scales. The interval scales shown in Fig. 11 all fall within a narrow range between −0.2 and 0.15. This means that 64% of the observers preferred the lightness-chroma adaptive algorithm over SDS and 56% preferred it over true-color when simultaneously considering all image content included in the experiment. This figure shows the SDS, chroma, and HCM algorithms appear to perform marginally worse than the true-color reference. Only the lightness-chroma adaptive algorithm has a slightly better performance than the true-color algorithm. Additional analyses indicated a high degree of image-de-

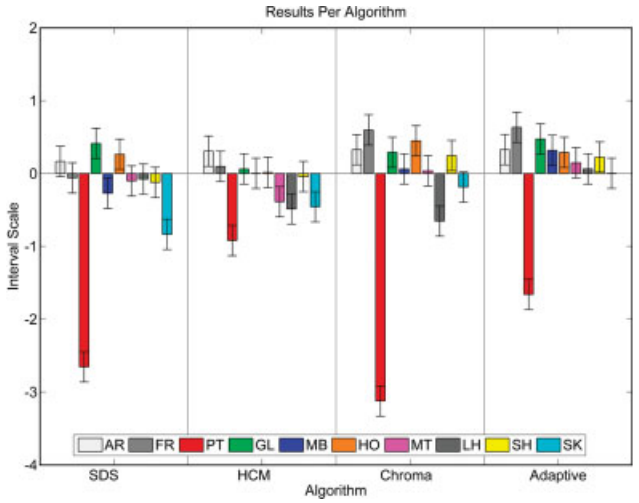

FIG. 12. Results across images for all observers in experiment A. The lightness-chroma adaptive algorithm is the only algorithm that, with one exception, has all values above zero, meaning it was the most robust algorithm relative to image content. Notice that the preference for the portrait image (PT), which corresponds to the red bar was very dependent on the algorithm. Note: PT in Fig. 12 is noted as PS in Fig. 9.

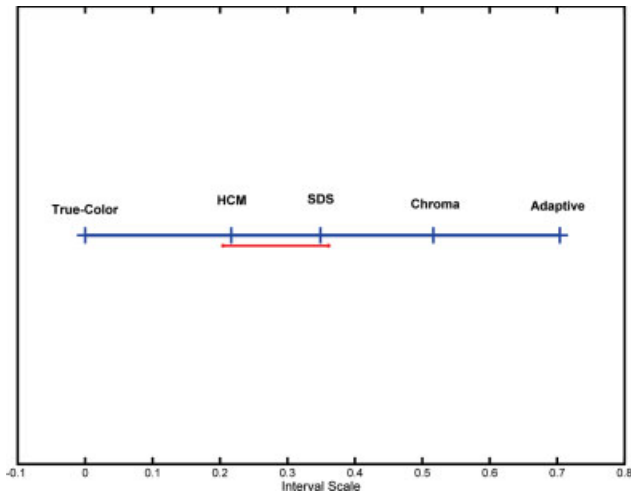

FIG. 13. Results for all images and observers in experiment B. The underlined portion represents algorithms that are not statistically different from each other. Only the HCM and SDS algorithms are statistically the same. In this figure, the results are more spread out (cf. Fig. 11), meaning observers were more consistent in their choices than in experiment A.

pendency in the preference scores. Therefore, the statistical meaning of the scale values shown in Fig. 11 is limited. Figure 12 shows the preference of each algorithm per image content. In this figure, there are four groupings containing the 10 image contents; each grouping is an algorithm. The results are scaled such that true-color has a value of 0 and hence results for that algorithm are not shown. The error bars correspond to 95% confidence intervals. Except for the portrait (PT) image, the lightness-adaptive algorithm always has values above zero, meaning that observers preferred images that were mapped using this algorithm over the true-color mapping. These figures further demonstrate that the lightness-adaptive extension method was the algorithm that was most consistently preferred over the true-color mapping.

Figure 13 shows the preference to the algorithms averaged over all participants and all image contents for experiment B. As before, the value associated with true-color mapping has been set to zero and thus serves as a reference solution. In other words, the interpretation of the interval scores is in terms of preference over true-color mapping. The results in Fig. 13 show that appropriate mapping on WG displays is significantly preferred over a true-color mapping. The lightness-chroma adaptive extension strategy is the most preferred method when averaged across all image contents. There was a more pronounced difference for experiment B between algorithms. The difference between Figs. 11 and 13 illustrates that images shown on the actual WG color display have different results than using algorithms on a simulated WG display. The maximum interval scale value in Fig. 13 is 0.7, which means that about 75% of observers preferred the lightness-chroma adaptive method over the true-color. In experiment A, and illustrated in Figs. 11 and 13, several GEAs were not preferred over a true-color mapping. This could be due to insufficient realism of the simulation instead of shortcomings in the algorithms. In the first experiment, the absolute difference between the gamuts was smaller because of the simulation on an EBU display. The differences amongst the algorithms should become more noticeable on an actual WG display since there is a larger difference in the actual gamuts.

Additional analysis revealed image dependency with the results, as seen in Fig. 14. Figure 14 shows the result of each image per algorithm in experiment B. Since the true-color algorithm was always set to zero, it

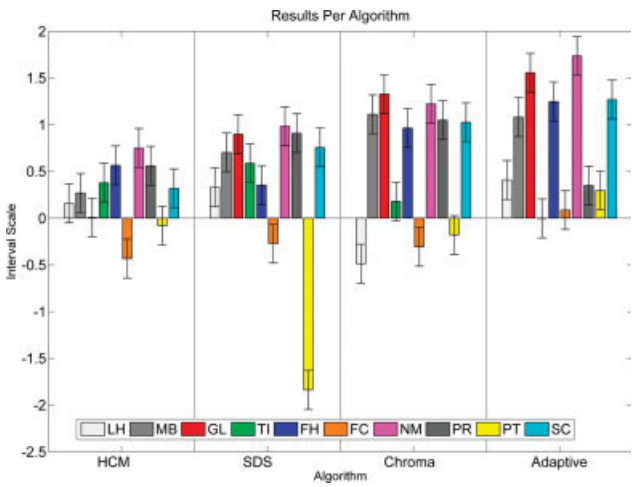

FIG. 14. Results for experiment B for all observers across images. Again, the lightness-chroma adaptive algorithm has all values above zero. The portrait image (yellow bar) was not as algorithm dependent as in Figure 13. Note: PT in Fig. 14 is noted as PS in Fig. 9. Likewise FC in Fig. 14 is noted as FR in Fig. 9.

is left out and any image score below zero is worse and any image above zero is better than true-color.

The content-dependency is particularly striking for the PT image, indicated by yellow bars in Fig. 14. The PT image depicts two Caucasian women and because none of the extension algorithms included explicit skin tone protection, gamut extension results in a less appreciated image. As mentioned earlier, lightness-chroma adaptive mapping was the most preferred method when averaged over all image contents and obtained the highest preference score for 7 of 10 image contents. Moreover, the lightness-chroma adaptive algorithm was the only method that consistently outperformed true-color mapping, as illustrated by its all positive preference values in Fig. 14.

CONCLUSIONS

Several gamut extension methods were developed and implemented as prototypes and their performance compared against a true-color mapping in two psychophysical experiments. The first experiment involved a WG simulation on a conventional display, whereas the second experiment was conducted on an actual WG display. In the first experiment, the performance of the five algorithms was similar when averaged over all 10 image-contents. In the second experiment, however, there were larger differences in preference observed among the extension methods. In this case, the reproduction gamut is substantially wider than the input gamut, such that the mapping strategies have a more pronounced effect on the appearance of the assessed stimuli. The lightness-chroma adaptive method was found to be the most preferred method and consistently outperformed the true-color mapping. Based on our observations, this prototype extension strategy is considered to be a promising and robust approach to gamut extension, especially when the algorithm is expanded with well-known solutions for protection of skin-tones and natural colors.

In spite of the promising outcome of the psychophysical studies, several challenges have yet to be overcome to apply gamut extension methods for WG displays successfully and robustly. First, observers often complained about certain colors in scenes being over-enhanced, resulting in an unnatural, fluorescent appearance of the colors on a WG display. To prevent the occurrence of such artifacts, the relationship between the maximum allowable saturation and the maximum acceptable brightness at these saturation levels should be investigated in more detail.

Second, the results of both psychophysical experiments exhibited strong dependencies of the algorithm performance toward image content. Although images were deliberately selected that were different in terms of content and color space coverage, a better understanding of how and why different image categories or types affect a given algorithm would be invaluable to algorithm developers. Finally, the GEAs considered in this work operate exclusively on pixel-based color coordinates. It is anticipated that the inclusion of additional modalities, such as spatial information or the development of image-adaptive approaches should lead to improved algorithms. Although the performance of the lightness-chroma adaptive method was promising in these experiments, it will be necessary to compare its merits against more advanced algorithms as they emerge.

ACKNOWLEDGMENTS

The authors thank the participants of the experiments for their time and comments, Ronald Kaptein and Roos Rajae-Joordens for their assistance in the analysis, Oleg Belik for providing the HCM function, and finally, many people within Philips Research who contributed invaluable comments and questions.

1. Morovic J, Luo MR. The fundamentals of gamut mapping: A survey. J Imaging Sci Technol 2001;45:283–290.
2. Fairchild M. Color Appearance Models, 2nd edition. Chichester, UK: Wiley-IS&T; 2005.
3. International Telecommunication Union, Radiocommunication Sector (ITU-R). Recommendation BT. 709-5:2002, Parameter values for the HDTV standards for production and international programme exchange, Geneva, Switzerland, 2002.
4. Kim M, Shin Y, Song YL, Kim I. Wide gamut multi-primary display for HDTV. Imaging and Vision, Proceedings of CGIV, Aachen, 2004. p 248–253.
5. Roth S, Ben-David I, Ben-Chorin M, Eliav D, Ben-David O. Wide gamut, high brightness multiple primaries single panel projection displays. SID Symp Dig 2003;34:118–121.
6. Sugiura H, Kaneko H, Kagawa S, Ozawa M. Six-primary-color 23-in WXGA LCD using six-color LEDs. SID Symp Dig 2005;36:1124–1127.
7. Sugiura H, Kaneko H, Kagawa S, Ozawa M. Prototype of a wide gamut monitor adopting an LED-backlighting LCD panel. SID Symp Dig 2003;34:1266–1269.
8. Sugiura H, Kaneko H, Kagawa S, Ozawa M, Tanizoe H. Wide-color-gamut monitors: LED-backlighting LCD and new phosphor CRT. Proc SPIE-Int Soc Opt Eng 2004;5289:151–160.
9. International Electrotechnical Commission (IEC). 61966-2-4. Multimedia systems and equipment—Colour measurement and management—Part 2–4: Colour management—Extended-gamut YCC colour space for video applications—xvYCC, Geneva, Switzerland, 2006.
10. Kang B, Morovic J, Luo MR, Cho M. Gamut compression and extension algorithms based on observer experimental data. ETRI J 2003;25:156–170.
11. Kotera H, Mita T, Hung-Shing C, Saito R. Image-dependent gamut compression and extension. Image Processing, Image Quality, Image Capture Systems Conference, Proceedings PICS, Montreal, 2001. Vol. 4, p 288–292.
12. Berns R. Billmeyer and Saltzman's Principles of Color Technology, 3rd edition. New York: John Wiley; 2000.
13. Sharma G. Digital Color Imaging Handbook. Boca Raton: CRC Press LLC; 2003.
14. Morovic J, Luo MR. Calculating medium and image gamut boundaries for gamut mapping. Color Res Appl 2000;25:394–401.
15. Thurstone LL. A law of comparative judgement. Psychol Rev 1927;34:273–286.
16. Rajae-Joordens RJE, Engel J. Paired comparisons in visual perception studies using small sample sizes. Displays 2005;26:1–7.